BIOCHEMISTRY
including biophysical chemistry & molecular biology

Article

pubs.acs.org/biochemistry

Structural Insights into the Mechanism of Four-Coordinate Cob(II)alamin Formation in the Active Site of the *Salmonella enterica* ATP:Co(I)rrinoid Adenosyltransferase Enzyme: Critical Role of Residues Phe91 and Trp93

Theodore C. Moore,[†] Sean A. Newmister,[‡] Ivan Rayment,*[,‡] and Jorge C. Escalante-Semerena*[,§]

[†]Department of Bacteriology and [‡]Department of Biochemistry, University of Wisconsin, Madison, Wisconsin 53706, United States
[§]Department of Microbiology, University of Georgia, Athens, Georgia 30602-2605, United States

Supporting Information

ABSTRACT: ATP:co(I)rrinoid adenosyltransferases (ACATs) are enzymes that catalyze the formation of adenosylcobalamin (AdoCbl, coenzyme B_{12}) from cobalamin and ATP. There are three families of ACATs, namely, CobA, EutT, and PduO. In *Salmonella enterica*, CobA is the housekeeping enzyme that is required for de novo AdoCbl synthesis and for salvaging incomplete precursors and cobalamin from the environment. Here, we report the crystal structure of CobA in complex with ATP, four-coordinate cobalamin, and five-coordinate cobalamin. This provides the first crystallographic evidence of the existence of cob(II)alamin in the active site of CobA. The structure suggests a mechanism in which the enzyme adopts a closed conformation and two residues, Phe91 and Trp93, displace 5,6-dimethylbenzimidazole, the lower nucleotide ligand base of cobalamin, to generate a transient four-coordinate cobalamin, which is critical in the formation of the AdoCbl Co−C bond. In vivo and in vitro mutational analyses of Phe91 and Trp93 emphasize the important role of bulky hydrophobic side chains in the active site. The proposed manner in which CobA increases the redox potential of the cob(II)alamin/cob(I)alamin couple to facilitate formation of the Co−C bond appears to be analogous to that utilized by the PduO-type ACATs, where in both cases the polar coordination of the lower ligand to the cobalt ion is eliminated by placing that face of the corrin ring adjacent to a cluster of bulky hydrophobic side chains.

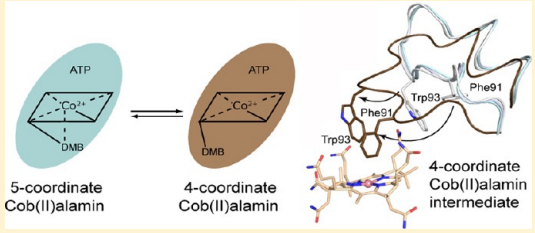

Cobalamin (Cbl, B_{12}) is one of the largest cofactors in biology and is utilized by organisms across all domains of life.[1,2] Cobalamin features a cobalt ion coordinated equatorially by the nitrogen atoms of a cyclic tetrapyrrole known as the corrin ring. The lower (Coα) axial ligand of Cbl is the purine analogue base 5,6-dimethylbenzimidazole (DMB), which is tethered to the corrin ring by a phosphodiester bond between an aminopropanol substituent of the ring and the phosphoryl moiety of the DMB-riboside monophosphate.[3]

In adenosylcobalamin (AdoCbl, coenzyme B_{12}, or CoB_{12}), the upper (Coβ) ligand is a 5′-deoxyadenosyl moiety covalently bound to the cobalt ion of the ring, forming a weak Co−C bond. Homolysis of the Co−C bond of AdoCbl results in five-coordinate cob(II)alamin and a 5′-deoxyadenosyl radical critical to the initiation of intramolecular rearrangements catalyzed by a variety of enzymes, such as ethanolamine ammonia-lyase,[4] diol dehydratase,[5] and methylmalonyl-CoA mutase,[6] among others.

AdoCbl is synthesized by a family of enzymes known as ATP:co(I)rrinoid adenosyltransferases (ACATs). There are three nonhomologous types of ACATs, CobA, PduO, and EutT, which were named on the basis of their function in the enterobacterium *Salmonella enterica*.[7−9] In this bacterium, CobA is the housekeeping ACAT involved in de novo AdoCbl synthesis and incomplete corrinoid salvaging.[7] CobA has the broadest substrate specificity of the three ACAT types and recognizes both complete and incomplete corrinoids.[10]

Corrinoid adenosylation proceeds via a reactive nucleophilic Co^+ species that is generated through a series of consecutive one-electron transfers to reduce the Co^{3+} ion.[11] The bacterial cytoplasm has sufficient reducing power for reduction of Co^{3+} to Co^{2+}, an event that removes the β-ligand.[12] Further reduction to Co^+ is thermodynamically difficult, because the $Co^{2+/+}$ redox couple in solution (−610 mV) is beyond the reach of known biological reductants.[13,14] ACATs raise the redox potential of the $Co^{2+/+}$ couple by generating a four-coordinate cob(II)alamin species in the active site.[15−17] In such species, the redox-active $3d_{z^2}$ orbital of cobalt is stabilized, resulting in an increase of ≥250 mV.[18] In such an environment, cob(II)alamin can accept an electron from reduced flavodoxin A (FldA), to generate cob(I)alamin.[12,19,20] Generation of cob(I)alamin is followed by a nucleophilic attack by Co^+ on the 5′-carbon of the ATP cosubstrate, forming AdoCbl and releasing tripolyphosphate (PPP_i).[21] This is accomplished in *Lactobacillus reuteri* PduO ACAT (hereafter *Lr*PduO) via

Received: October 9, 2012
Revised: November 13, 2012
Published: November 14, 2012

   dx.doi.org/10.1021/bi301378d | *Biochemistry* 2012, 51, 9647−9657

placement of the lower ligand coordination site of the cobalt ion in a hydrophobic environment.[35] In *Lr*PduO, Phe112 displaces DMB from its coordination bond with the cobalt ion to generate the four-coordinate intermediate.[23] It was unknown whether this mechanism is shared by other nonhomologous ACATs or whether each ACAT has a distinct mechanism for achieving a four-coordinate cob(II)alamin.

CobA is capable of generating the four-coordinate intermediate;[18] however, such an intermediate has not been observed in the active site of CobA, so that the mechanism for the conversion of five- to four-coordinate cob(II)alamin in CobA was unknown. In earlier structural studies, prior to learning about the importance four-coordinate cob(II)alamin intermediates, CobA was crystallized in complex with HO-cob(III)alamin (HOCbl).[22] In that structure, the cobalt ion of HOCbl is not in a suitable position for nucleophilic attack because it is located too far (>6 Å) from the 5′-carbon of ATP.[22] Significantly, HOCbl is a Co^{3+} species that is not encountered by the enzyme in vivo.[12]

To address the mechanism by which four-coordinate Cbl formation is supported in CobA, we have determined the structure of CobA in complex with cob(II)alamin and MgATP at 2.0 Å resolution. This revealed tetradentate coordination for the cobalt ion and provided insight into how this is accomplished in this class of ACATs. The structure was used to guide an investigation in vivo and in vitro of the components of the active site that appear to be critical for function.

MATERIALS AND METHODS

Strains, Culture Media, and Chemicals. Strains used in this study are listed in Table S1 of the Supporting Information. Primers used for polymerase chain reaction-based site-directed mutagenesis are listed in Table S2 of the Supporting Information. Chemicals were purchased from Sigma and were used without further purification.

Minimal medium[24] containing ethanolamine as a carbon, energy, and nitrogen source was used to assess AdoCbl biosynthesis via the adenosylcobalamin-dependent expression of the ethanolamine utilization (*eut*) operon of *S. enterica* sv. Typhimurium strain LT2 as described previously.[7] The culture medium was supplemented with ethanolamine (90 mM), glycerol (0.5 mM), methionine (2 mM), $MgSO_4$ (1 mM), arabinose (0.5 mM), and trace minerals.[25] AdoCbl precursors dicyanocobinamide [$(CN)_2$Cbi, 100 nM] and 5,6-dimethylbenzimidazole (DMB, 300 μM) were also added to the medium. Lysogenic broth (LB)[26,27] and Nutrient Broth (Difco Laboratories) were used as complex media.

Protein Overproduction and Purification. Overproduction and purification of tagless, wild-type CobA ($CobA^{WT}$) protein were performed as described previously.[22] $CobA^{WT}$ was concentrated [10000 molecular weight cutoff (MWCO) centrifugal filter, Millipore] to 20 mg/mL as determined by A_{280} using the calculated molar extinction coefficient (23950 M^{-1} cm^{-1}, ExPASy[28]). The protein was flash-frozen in liquid nitrogen and stored at −80 °C until it was used.

To facilitate overproduction and purification of CobA variants, the *S. enterica* $cobA^+$ allele was cloned into a pTEV5 vector to direct synthesis of CobA proteins fused to an N-terminal, rTEV protease-cleavable H_6 tag.[29] Mutant *cobA* alleles were constructed using the QuickChange II site-directed mutagenesis kit (Stratagene). The presence of the desired mutations was confirmed using BigDye Terminator DNA sequencing protocols (ABI PRISM); reaction mixtures were resolved at the University of Wisconsin Biotechnology Center. Plasmids directing the synthesis of the CobA variants were moved by electroporation into a strain of *Escherichia coli* BL21(λDE3) carrying a null allele of *btuR*, the *cobA* homologue in this bacterium (Table S1 of the Supporting Information). Strains expressing different *cobA* alleles were inoculated into 2 L of LB containing ampicillin (100 μg/mL) and grown while being shaken at 37 °C to an OD_{600} of ∼0.6. At that point, the incubator temperature was decreased to 15 °C for 30 min before overnight induction with 1 mM IPTG. Cells were harvested (9000*g* for 15 min at 4 °C) and stored at −80 °C for at least 3 days. Cell pellets were resuspended in 100 mM tris(hydroxymethyl)aminomethane hydrochloride buffer (Tris-HCl) (pH 8 at 4 °C) with 500 mM NaCl, 70 mM imidazole, 1 mM tris(2-carboxyethyl)phosphine (TCEP), and protease inhibitor cocktail (Sigma) at a density of 3 mL of buffer per gram of cell pellet. Resuspended cells were lysed by two passes through a French pressure cell (10.3 MPa) at 4 °C. The insoluble fraction was removed by centrifugation (44000*g* for 45 min at 4 °C) followed by filtration through a 0.45 μm filter (Millipore). Clarified lysate was applied over a Ni-activated nitrilotriacetic acid (NTA) column (5 mL of HisPur resin, Thermo). After being loaded, the column was washed with 5 bed volumes of buffer A [100 mM Tris-HCl (pH 8 at 4 °C)] containing 500 mM NaCl, 70 mM imidazole, and 1 mM TCEP. CobA protein bound to the resin was eluted using 5 bed volumes of buffer B (buffer A containing 500 mM imidazole) and collected in 3 mL fractions. The location of CobA was established by sodium dodecyl sulfate−polyacrylamide gel electrophoresis (SDS−PAGE) analysis of fractions. Fractions containing high-purity CobA (12 mL) were combined and dialyzed (10000 MWCO, Pierce) with His_7-tagged recombinant tobacco etch virus (His7-rTEV) protease (1 mg/mL, 1:50, v/v) to cleave the His_6 tag. His_7-tagged rTEV was prepared as described elsewhere.[30] The combined fractions were dialyzed against buffer C (buffer A containing 20 mM imidazole) with three buffer changes at 4 °C. The first and second dialyses lasted 3 h, and the third dialysis lasted 10 h. The dialyzed fractions were loaded onto a fresh Ni-NTA column and washed with 5 bed volumes of buffer A; the flow-through was collected in 3 mL fractions. The protein content of these fractions was analyzed by SDS−PAGE; those containing CobA of the highest purity were pooled (9 mL) and dialyzed against 1 L of 50 mM Tris-HCl (pH 8.0, 4 °C), 500 mM NaCl, 1 mM TCEP, and 10% (v/v) glycerol at 4 °C. Three changes of dialysis buffer were used at 4 °C. The first and second lasted 3 h, and the third lasted 10 h. The final dilution factor of the dialyzable material was 7.2×10^{-7}. Proteins were concentrated (10000 MWCO centrifugal filter, Millipore); the concentration was measured by A_{280} using the calculated molar extinction coefficients (Table S3 of the Supporting Information, ExPASy), and the proteins were flash-frozen in liquid N_2 and stored at −80 °C. Flavodoxin A (FldA) and ferredoxin (flavodoxin):$NADP^+$ reductase (Fpr) were produced and purified as described previously.[12]

Crystallography. Crystallization conditions were analyzed using a 144-condition sparse matrix screen developed in the Rayment laboratory. All crystals of tagless CobA were grown by hanging-drop vapor diffusion in an anoxic chamber (Coy) at 20−25 °C. CobA was thawed and dialyzed three times against 1 L of 20 mM Tris-HCl (pH 8.0, 25 °C) for 30 min each at 25 °C to remove glycerol. A reaction mixture containing 20 μg/mL Fpr, 20 mM NADH, 3 mM ATP, 4.5 mM $MgCl_2$, and 2 mM HOCbl was constituted at room temperature inside an

dx.doi.org/10.1021/bi301378d | *Biochemistry* 2012, 51, 9647−9657

anoxic chamber (90% N_2/10% H_2) to reduce HO-cob(III)alamin to cob(II)alamin. The reduction was performed inside the anoxic chamber to prevent the rapid oxidation of cob(II)alamin to cob(III)alamin. Anoxic CobA was added to the reaction mixture after preincubation for 20 min at 25 °C. The final concentration of CobA in the mixture was 10 mg/mL. CobA was cocrystallized with MgATP and cob(II)alamin by mixing 2 μL of the reaction mixture with 2 μL of well solution composed of 100 mM 2-(*N*-morpholino)ethanesulfonic acid (MES) (pH 6.0), 320 mM NaCl, and 19.6% (w/v) polyethylene glycol 4000 (PEG4000).

Brown, orthorhombic crystals (0.1 mm × 0.5 mm) were observed after 48 h. The crystals were incrementally transferred in two steps to a cryoprotectant solution that contained 22.5% (w/v) PEG4000, 13.8% (v/v) ethylene glycol, 100 mM MES (pH 6.0), 240 mM NaCl, 0.5 mM HOCbl, 20 μg/mL Fpr, 10 mM NADH, 1 mM ATP, and 1.5 mM $MgCl_2$ in acrylic batch plates inside the anaerobic chamber. The plates containing the crystals were moved into an O_2-free argon bath for ease of manipulation before being frozen. The crystals were briefly exposed to oxygen (≤1 s) while being flash-frozen in liquid nitrogen. Tagless CobA in complex with MgATP and cob(II)alamin crystallized in space group $P2_12_12_1$ with one homodimer of CobA per asymmetric unit and the following unit cell dimensions: a = 59.7 Å, b = 74.2 Å, c = 92.4 Å. Each chain contained ATP; one chain contained four-coordinate cob(II)alamin, and the other contained five-coordinate cob(II)alamin.

X-ray Data Collection and Structure Refinement. X-ray data for the CobA·cob(II)alamin·MgATP complex were collected at 100 K on Structural Biology Center beamline 19BM at the Advanced Photon Source (Argonne National Laboratory, Argonne, IL). Diffraction data were integrated and scaled with HKL3000.[31] Data collection statistics are listed in Table 1. The structure of the CobA·cob(II)alamin·MgATP complex was determined using the apo form of CobA (Protein Data Bank entry 1G5R)[22] as a molecular replacement search model in Molrep.[32] The final model was generated with alternate cycles of manual model building and least-squares refinement using Coot[33] and Refmac.[34] Refinement statistics are listed in Table 1.

In Vivo Assessment of CobA Variant Function. Mutant *cobA* alleles encoding specific CobA variants were constructed on plasmid pCOBA70 (Table S2 of the Supporting Information) using the QuickChangeII site-directed mutagenesis kit (Stratagene). Plasmids carrying mutant *cobA* alleles were moved by electroporation into a strain harboring a null allele of *cobA* [JE15023 (Table S1 of the Supporting Information)]. The functionality of CobA variants was assessed in vivo for their ability to restore AdoCbl synthesis in a Δ*cobA* strain during growth on ethanolamine as the sole source of carbon, energy, and nitrogen. Strains were grown to full density overnight in Nutrient Broth with ampicillin (100 μg/mL). A 20 μL sample was used to inoculate fresh minimal medium containing ethanolamine, $(CN)_2$Cbi, and DMB (1:40, v/v) in 96-well plates; each culture was analyzed in triplicate. Growth behavior was monitored for 48 h using a BioTek ELx808 Ultra microplate reader. Data were collected at 630 nm every 1800 s at 30 or 37 °C. Plates were shaken for 1795 s between readings.

In Vitro Assessment of CobA Variant Function. Continuous spectrophotometric assays of CobA activity were performed using either cob(II)alamin or cob(I)alamin substrate as described previously,[23,35] with the following modifications.

Table 1. Data Collection and Refinement Statistics for the CobA·ATP·B12 Complex[a]

space group	$P2_12_12_1$
wavelength (Å)	0.979
resolution range	50−1.95 (1.98−1.95)
no. of measured reflections	647369
no. of unique reflections	30580
redundancy	4.7 (4.8)
completeness (%)	98.4 (99.8)
average I/σ	29.4 (3.6)
R_{merge} (%)[b]	9.1 (73.2)
R_{work}[c]	17.8
R_{free}[c]	23.0
no. of protein atoms	2769
no. of ligand atoms	225
no. of water molecules	332
average B factor (Å^2)	33.989
Ramachandran plot (%)	
most favored	97.8
allowed	2.2
disallowed	0.0
root-mean-square deviation	
bond lengths (Å)	0.020
bond angles (deg)	2.657

[a]Values in parentheses are for the highest-resolution shell. [b]$R_{merge} = \sum|I_{(hkl)} - I| \times 100/\sum|I_{(hkl)}|$, where the average intensity I is taken over all symmetry equivalent measurements and $I_{(hkl)}$ is the measured intensity for a given observation. [c]$R_{factor} = \sum|F_o - F_c| \times 100/\sum|F_o|$, where R_{work} refers to the R_{factor} for the data utilized in the refinement and R_{free} refers to the R_{factor} for 5% of the data that were excluded from the refinement.

All reaction mixtures contained 0.2 M Tris-HCl (pH 8, 37 °C), 1.5 mM $MgCl_2$, 0.5−50 μM HOCbl, and 1−1000 μM ATP. Two assays were used to quantify CobA activity: (i) the Co^+ assay, in which 0.5 mM Ti(III)citrate was used to reduce cob(III)alamin to cob(I)alamin, and (ii) the Co^{2+} assay. The reaction mixture of this assay included 44 μg/mL Fpr, 300 μg/mL FldA, and 1 mM NADH to reduce cob(III)alamin to cob(II)alamin.[36] CobA-dependent formation of AdoCbl was monitored using a Perkin-Elmer Lambda 45 UV/vis spectrophotometer.

RESULTS AND DISCUSSION

Evidence of the Existence of Four-Coordinate Cob(II)alamin in the Active Site of CobA. CobA was crystallized under anoxic conditions in the presence of cob(II)alamin in an effort to generate a structure of the enzyme with the physiologically relevant substrate in its active site. The structure of the CobA·cob(II)alamin·MgATP complex was determined at 2.0 Å resolution; its overall fold is shown in Figure 1. The protein crystallized with a dimer in the asymmetric unit. The electron density is well-defined for both subunits in the dimer. The final model extends continuously from amino acid Tyr6 to Tyr196 for subunit A and from Arg28 to Tyr196 for subunit B. The polypeptide chain exhibits an α/β-fold similar to that seen in RecA, F_1ATPase, and adenosylcobinamide kinase/adenosylcobinamide guanylyltransferase,[22] where a P-loop is located at the end of the first β-strand. Both active sites contain unequivocal electron density for MgATP and a corrinoid (Figure 2). As noted in the original structure for CobA, MgATP is oriented in a unique manner in the opposite direction across the P-loop compared to that seen in other

dx.doi.org/10.1021/bi301378d | *Biochemistry* 2012, 51, 9647−9657

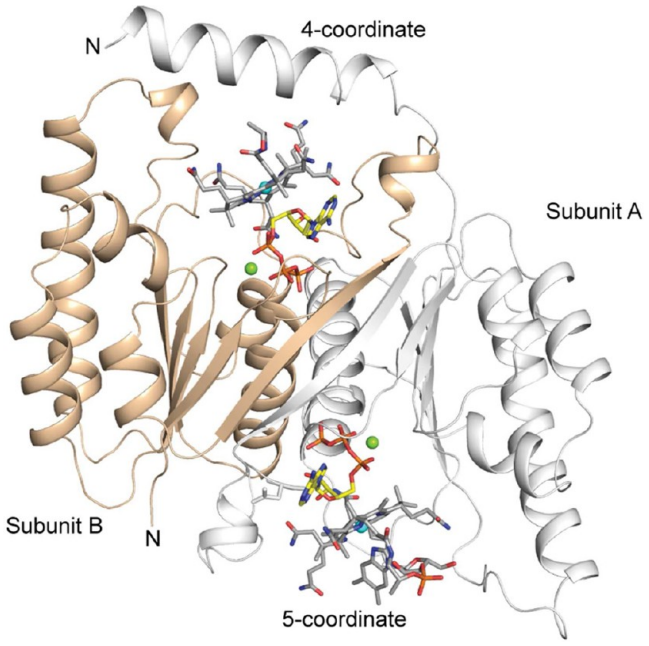

Figure 1. Cartoon representation of the *S. enterica* CobA homodimer. Each subunit binds one molecule of MgATP and one molecule of cob(II)alamin. Subunit B (colored wheat) binds a four-coordinate cob(II)alamin, whereas subunit A (colored white) binds a five-coordinate cob(II)alamin. The N-terminal helix of subunit A extends over the active site of subunit B, while the N-terminal helix of subunit B is disordered. Figures 1−5 were prepared with Pymol.[44]

enzymes with this fold.[22] In this way, the γ-phosphate resides at the location normally occupied by the α-phosphate in other nucleotide hydrolases. This facilitates the transfer of the 5′-carbon of the ribose to the cobalt ion.

The earlier structure of the CobA·hydroxycob(III)alamin·MgATP complex also crystallized with a molecular dimer in the crystallographic asymmetric unit, where both active sites contained MgATP but only one bound cob(III)alamin. In the latter case, the N-terminal section of the polypeptide chain from the symmetry-related subunit folded over the cobalamin and DMB remained bound to the central cobalt ion. In this way, sections of both subunits of the dimer contributed to the active site. Conversely, the corresponding section of the opposing polypeptide chain was disordered in the active site that lacked hydroxycob(III)alamin. In the crystal structure presented here, there is also a dimer in the asymmetric unit but both active sites include cob(II)alamin and MgATP, but even here there is asymmetry in the molecular dimer, as described below.

In the structure of the CobA·cob(II)alamin·MgATP complex, one site is occupied by four-coordinate cob(II)alamin while the other site is occupied by five-coordinate cob(II)alamin. In the active site that contains the four-coordinate cob(II)alamin (subunit B), the N-terminal helix of subunit A folds over the corrin ring and contributes to the displacement of the lower ligand (DMB). In this active site, there is no electron density visible for the aminopropanol linkage, nucleotide loop, or DMB, but the remainder of the corrin ring is well-defined (Figure 2A). Presumably, the missing

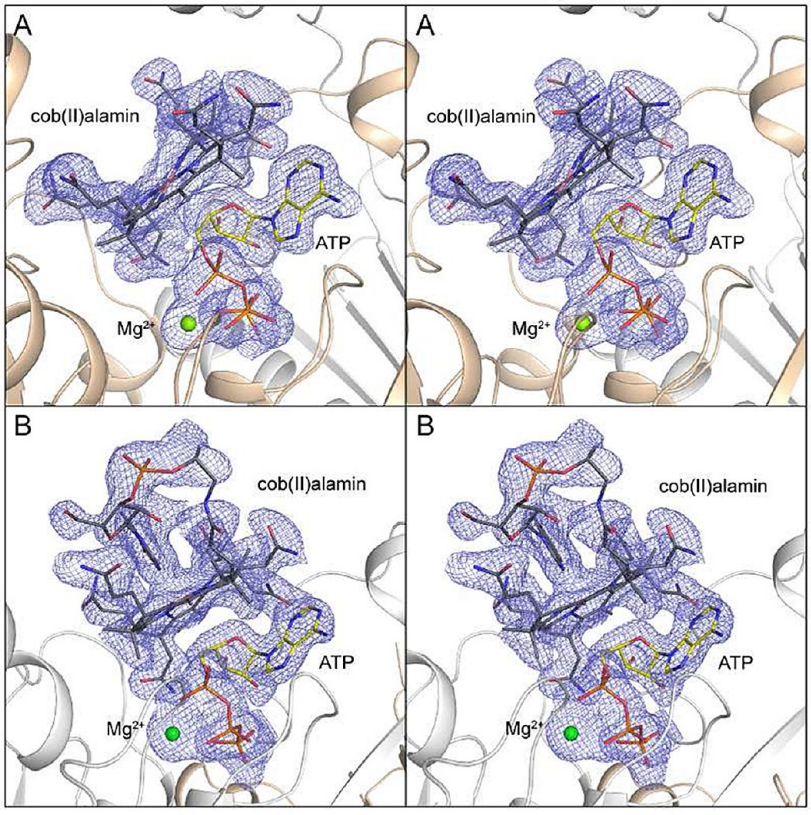

Figure 2. Stereoview of the electron density for four-coordinate cob(II)alamin (A), five-coordinate cob(II)alamin (B), and MgATP. Electron density [2.0σ for four-coordiante cob(II)alamin and MgATP, 1.5σ for five-coordinate cob(II)alamin] was calculated from coefficients of the form $F_o - F_c$, where cob(II)alamin and MgATP were omitted from phase calculation and refinement. The electron density was not as well-defined in the five-coordinate active site.

dx.doi.org/10.1021/bi301378d | *Biochemistry* 2012, 51, 9647−9657

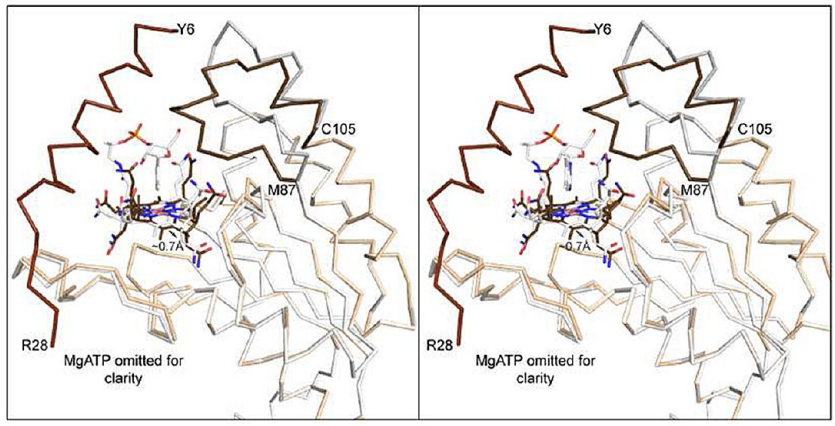

Figure 3. Comparison of the polypeptide chain and cob(II)alamin for the four- and five-coordinate states. This shows a stereoribbon representation of the superposition of the four- and five-coordinate states. The four-coordinate state is colored wheat and brown and is denoted as the "closed" conformation of the protein. The five-coordinate species is colored white and light gray and is denoted as the "open" conformation of the protein. The protein fold is essentially identical for both subunits except for the N-terminal helix that is ordered in subunit A and a loop between Met87 and Cys105 (colored brown and gray in the closed and open states, respectively). This loop is well-ordered in both active sites but rotates to exclude DMB in the four-coordinate state. MgATP was excluded for the sake of clarity.

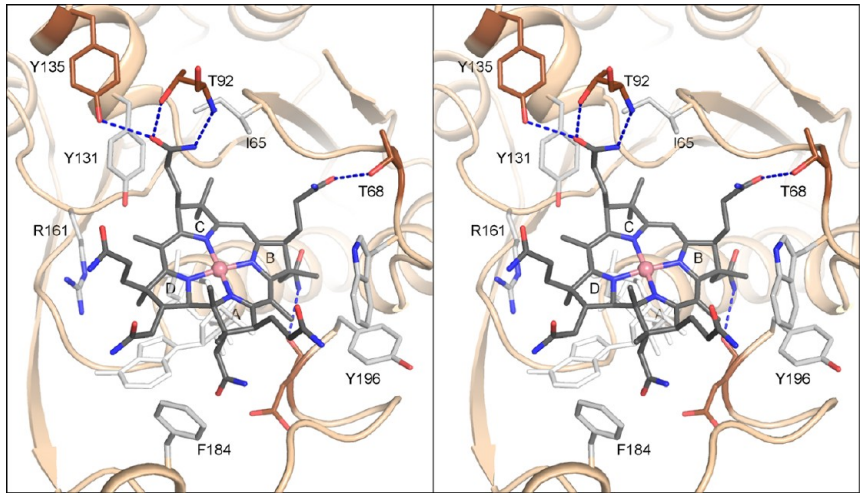

Figure 4. Stereoview of the corrin binding site for four-coordinate cob(II)alamin. The corrin ring sits across the MgATP and interacts with a constellation of polar and hydrophobic side chains around the periphery of the corrin ring. The large hydrophobic side chains are colored gray.[22] The loop that extends over the corrin ring and displaces DMB in the five-coordinate state (Ala88–Asn97) was omitted for the sake of clarity.

segments of cob(II)alamin are solvent-exposed and do not contribute to substrate binding. This observation is consistent with the broad specificity of CobA and its role as a corrinoid salvaging enzyme. The square-planar structure of the Co(II) ion and its four nitrogen ligands from the corrin ring together with the lack of axial ligands reveal the presence of four-coordinate cob(II)alamin. A similar structure was observed in the active site of the *L. reuteri* PduO (*Lr*PduO) ACAT.[23]

In contrast, the other active site (subunit A) contains a five-coordinate cob(II)alamin. Here, the DMB ligand remains coordinated via N3 to the central Co(II) ion. Additionally, the N-terminal helix from opposing subunit B is disordered and could not be modeled because of the lack of electron density. The electron density level for the ligands in this active site is somewhat lower than that observed in the four-coordinate site, suggesting a lower occupancy. Nevertheless, the density for DMB is well-defined, although that for the aminopropanol arm and nucleotide loop is less continuous, suggesting conformational flexibility in the absence of the N-terminal helix from the opposing subunit (Figure 2B).

Interactions of the Corrin Ring with Side Chains in the Active Site. The protein cores of the two subunits in the asymmetric unit are highly similar and show a root-mean-square difference of only 0.19 Å between 129 structurally equivalent α-carbon atoms. The only significant differences occur in the regions that interact with the corrin ring and relate to differences between the four and five coordination of cob(II)alamin. These differences are discussed later. Overall, the corrin ring binds in a similar location in both active sites but is shifted ~0.7 Å further into the binding pocket in the case of the four-coordinate cob(II)alamin (Figure 3). In both active sites, the corrin ring lies on top of the MgATP so that most of the interactions occur around the periphery of the corrinoid. The four-coordinate cob(II)alamin experiences more interactions than the five-coordinate cob(II)alamin as a consequence of the displacement of DMB and the small movement further into the active site. However, the interactions in the

dx.doi.org/10.1021/bi301378d | *Biochemistry* 2012, 51, 9647–9657

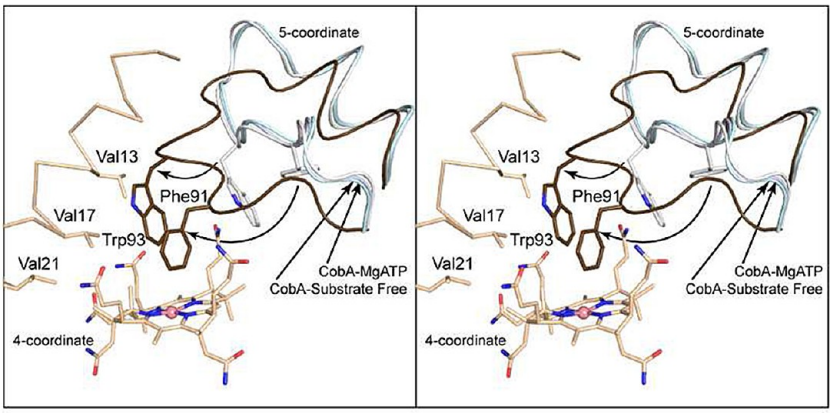

Figure 5. Stereo view of the conformational change between the open and closed states of CobA for the loop between Met87 and Cys105. This shows a superposition of the four-coordinate cob(II)alamin closed state and the open state observed in the five-coordinate complex. The closed state is colored wheat and brown, whereas the open state of the cob(II)alamin complex is colored white. The conformation of Met87−Cys105 is also seen in the MgATP and substrate free CobA determined previously.[22] The loops for these structures are colored light cyan and blue, respectively. In the closed state, Phe91 and Trp93 rotate and translate from a partially buried location within the loop to a stacking position ∼4 Å above the corrin ring. The side chains for Phe91 and Trp93 move by ∼12.1 and 7.5 Å, respectively. The ordered N-terminal helix from the opposing helix is colored wheat for the closed complex. This contributes three hydrophobic side chains to the corrin binding pocket. The coordinates for the structures of MgATP and substrate free CobA were taken from Protein Data Bank entries 1G5T and 1G5R, respectively.

five-coordinate species are also found in the four-coordinate site.

There are a very limited number of direct polar interactions with the corrin ring. In both coordination states, there is a hydrogen bond between the carbonyl oxygen of Asp195 and the acetamide group on the β-face of pyrrole ring B and a hydrogen bond between Oγ of Thr68 and the propionamide group on the α-face of pyrrole ring B (Figure 4). The interaction between Asp195 and the acetamide group on the β-face of pyrrole ring B was present in the previously reported structure.[22] In the four-coordinate state, there are several additional polar interactions, which include hydrogen bonds between the α-face propionamide of pyrrole ring C and the hydroxyl of Tyr135, Oγ of Thr92, and amide hydrogen of Thr92. A hydrogen bond is also formed between the amide hydrogen of Thr68 and the α-face propionamide of pyrrole ring B. Apart from these specific interactions, there are numerous water-mediated interactions with the remaining polar groups on the corrin ring. It is likely that this ensemble of polar interactions provides conformational specificity, but most of the binding energy is probably derived from the hydrophobic components of the binding site.

A constellation of hydrophobic residues and hydrophobic components of polar side chains surrounded the corrin ring (Figure 4). The hydrophobic nature of the binding site was noted in the earlier structure of CobA complexed with hydroxycob(III)alamin, though most of those residues were not in contact with the corrinoid because the cobalt ion was positioned ∼6.1 Å from the 5′-carbon of ATP. This distance was presumed to be due to the hydroxyl β-ligand, which was not visualized in the crystal structure but helped explain why the substrate did not bind in the hydrophobic active site. In this structure, the corrin ring is nestled more deeply in the binding pocket and is in the proximity of Ile65, Trp69, Arg161, Phe184, and Tyr196. This serves to bring the Co(II) ion significantly closer to the MgATP. In the current structure, the Co(II) ion is 3.1 Å from its target and is well-positioned to initiate nucleophilic attack once it is reduced to cob(I)alamin.[37] This closer positioning of the corrin ring to MgATP seen in the Co(II) state compared to that in the Co(III) state is solely due to the reduction of the cobalt ion and not due to displacement of the lower ligand to attain the four-coordinate state because five-coordinate cob(II)alamin adopts a similar position (Figure 3). It is highly unlikely that a hydroxyl group or water molecule could fit within this space as hypothesized with the earlier CobA·cob(III)alamin structure.

Computer-predicted modeling indicated that the terminal electron donor protein, FldA, binds closed-conformation CobA at Arg9, Arg98, and Arg195 and also has undermined interactions with the N-terminal helix of the adjacent subunit.[19] This positions the dihydroflavin of FldA in the proximity of a solvent-accessible patch near pyrrole rings B and C of bound four-coordinate cobalamin. The route by which the terminal electron is delivered from FldA to CobA is unknown, but it is possible that corrin accessibility through this patch is needed for cobalamin reduction.

Structural Basis for the Formation of Four-Coordinate Cob(II)alamin. In the four-coordinate state, the lower ligand (DMB) and entire nucleotide arm are displaced by Phe91 and Trp93 and the N-terminal helix from the opposing subunit (Figure 5). This yields a closed active site or conformation for the enzyme. Relative to the five-coordinate cob(II)alamin state, this displacement involves a conformational change in the loop that extends from Met87 to Cys105 and includes a change in the orientation of Phe91 and Trp93. The structure of this loop in the five-coordinate state is essentially identical to that seen in the substrate free and MgATP-bound forms reported earlier (Figure 5).[22] In this case, the active site adopts an open conformation. This suggests that the active site can adopt two stable conformational states, the first of which (open) arises in the absence of substrate, in the presence of MgATP, and in the five-coordinate state. The second conformation (closed) occurs only with four-coordinate cob(II)alamin. Examination of the crystal lattice for the current structure indicates that the active site that carries the five-coordinate cob(II)alamin complex is maintained in the open state by crystal packing forces and thus neither implies nor excludes negative cooperativity between the active sites.

dx.doi.org/10.1021/bi301378d | *Biochemistry* 2012, 51, 9647−9657

As shown in Figure 5, Phe91 and Trp93 move a considerable distance during the transition from the open to the closed conformation. The α-carbons of these residues move 7.1 and 5.1 Å, respectively, whereas the side chains themselves move ~12.1 and 7.5 Å, respectively (Figure 5). Interestingly, these side chains are mostly buried in both the open and closed conformations, suggesting that there is a small difference in hydrophobic stabilization between states. Thus, in the closed state, the Co(II) is placed in a hydrophobic environment that serves to eliminate water from the α-face of the corrin ring that would quench the cob(I)alamin nucleophile.[38] The aromatic side chains of residues 91 and 93 are approximately orthogonal to the corrin ring in the closed conformation. This orientation makes π−π stacking with the corrin ring unlikely, although these residues might be stabilizing cobalamin via π−σ interactions.[40]

The N-terminal helix of the adjacent subunit provides additional hydrophobic cover to the α-face of the corrin ring. The side chains of Val13 and Val17 abut the face of Trp93, whereas Val21 contacts the hydrophobic component of the α-propionamide on pyrrole ring A (Figure 5).

The structure of the four-coordinate substrate suggests that Phe91 and Trp93 play a critical role in CobA function. This role was tested by site-directed mutagenesis. Both in vitro and in vivo analyses were performed, as each provided unique information about the contribution of these residues to adenosyltransferase activity. The in vivo analysis is a sensitive test of the ability of a variant to produce adenosylated corrinoid, as only small amounts are needed for growth. However, the in vivo analysis cannot distinguish between problems of protein expression and folding versus a lack of enzymatic activity. The biochemical analysis provides insight into the molecular consequences of a mutation but does not necessarily indicate how it might influence the biological fitness of its host. The effects of mutations on in vivo function are described first.

Residues Phe91 and Trp93 Are Critical for the Function of CobA in Vivo. A series of mutant *cobA* alleles were constructed and placed under the control of an inducible promoter for expression, and the resulting variant proteins were tested for their ability to restore AdoCbl synthesis in a Δ*cobA* strain in vivo. *S. enterica* cannot synthesize AdoCbl de novo under aerobic conditions[1] but can scavenge incomplete corrinoids. AdoCbl is required for induction of the *eut* operon in *S. enterica*, which allows the strain to catabolize ethanolamine as a carbon, nitrogen, and energy source.[39] The precursor Cbi was added to the medium instead of Cbl to prevent false positives via the Cbl-specific ACAT, EutT. CobA is capable of adenosylating Cbi and Cbl.[7] AdoCbi proceeds via *S. enterica*'s corrinoid salvaging pathway to become AdoCbl.[1]

Variant CobA proteins with conservative substitutions at these positions (i.e., F91Y, W93F, and W93Y) retained sufficient activity to support AdoCbl synthesis at 37 °C, resulting in wild-type growth of the Δ*cobA* strain (Figure 6A, group 1). Interestingly, a variant in which residues Phe91 and Trp93 were switched (i.e., CobA$^{F91W,\ W93F}$) also retained sufficient activity to support AdoCbl synthesis at 37 °C (Figure 6A, group 1). Notably, variant CobA^{W93H} only partially restored growth of the Δ*cobA* strain at 37 °C (Figure 6A, group 2). When the growth temperature was lowered to 30 °C, CobA^{W93H} supported growth of the Δ*cobA* strain to full density after a short lag and at a slightly slower growth rate (Figure 6B, group 2). In contrast, alanine substitutions at residue Phe91 or Trp93 abolished growth (Figure 6A,B, group 3).

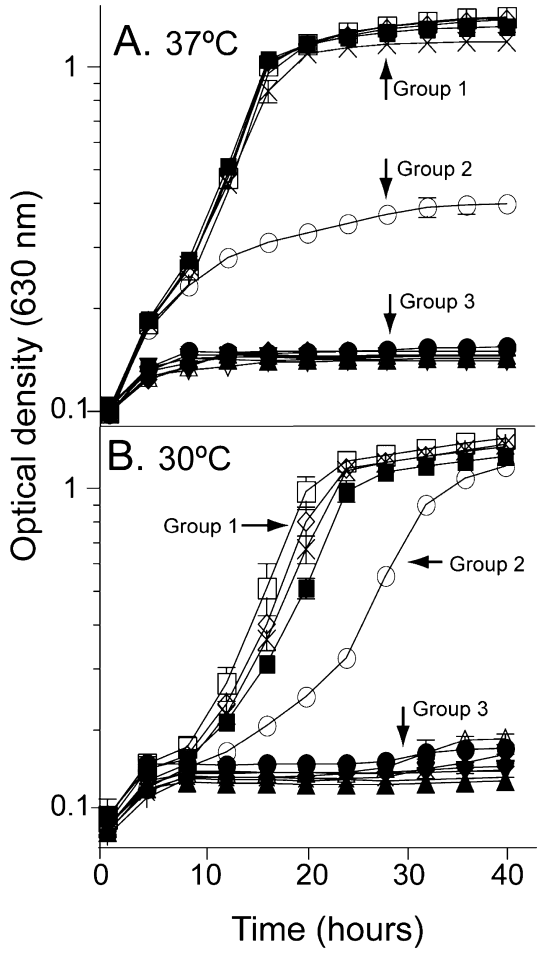

Figure 6. Representative growth of Δ*cobA* strains expresssing variant CobA proteins on a plasmid. The medium contained ethanolamine as the sole source of carbon, nitrogen, and energy and was supplemented with $(CN)_2$Cbi and DMB at 37 (A) and 30 °C (B), respectively. Strains synthesizing variant CobAs are grouped according to the maximal OD reached under these conditions. Group 1: CobA^{WT} (■), CobA^{F91Y} (□), CobA^{W93F} (△), CobA^{W93Y} (×), and CobA^{F91W,W93F} (bars). Group 2: CobA^{W93H} (○). Group 3: vector control (▲), CobA^{F91A} (▼), CobA^{F91W} (◆), CobA^{F91H} (○), CobA^{F91D} (△), CobA^{W93A} (▽), CobA^{W93D} (+), and CobA^{F91A,W92A} (∗). Figures 6 and 7 were made using Prism 4 (GraphPad, 2003).

Residues Phe91 and Trp93 Are Needed To Displace the Lower Ligand of Five-Coordinate Cob(II)alamin. In general, CobA variants that synthesized enough AdoCbl to support growth of a Δ*cobA* strain on ethanolamine had specific activities similar to that of the wild-type enzyme (Figure 7B) with two exceptions that are discussed below. All CobA variants that supported growth of the Δ*cobA* strain on ethanolamine had substitutions that retained aromatic side chains. On the basis of the structure reported here, and extensive analysis of the mechanism of the *Lr*PduO ACAT, we suggest that hydrophobic side chains at positions 91 and 93 play a role in the conversion of five- to four-coordinate cob(II)alamin to allow the formation of the cob(I)alamin nucleophile. In support of this hypothesis, alanine substitutions at either Phe91 or Trp93 resulted in variant enzymes that are unable to produce sufficient AdoCbl for growth on ethanolamine.

dx.doi.org/10.1021/bi301378d | *Biochemistry* 2012, 51, 9647−9657

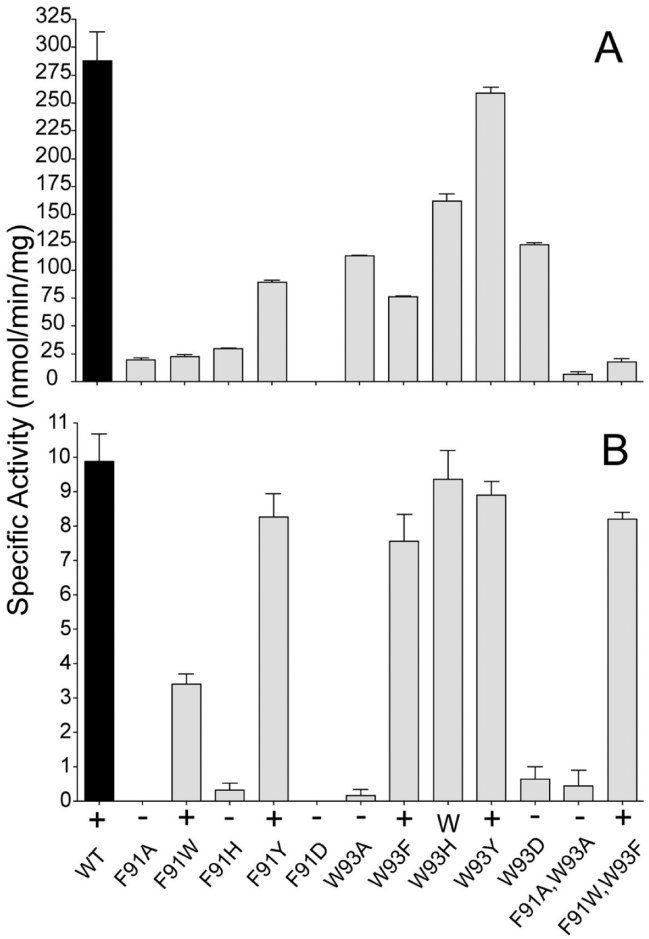

Figure 7. In vitro and in vivo assessment of CobA variant function. Shown are specific activities when cob(I)alamin (A) or cob(II)alamin (B) was the substrate. Plus and minus signs indicate whether a Δ*cobA* strain synthesizing a plasmid-encoded CobA variant could reach an OD_{630} of ≥0.2 after incubation with ethanolamine medium for 24 h at 37 °C. The W symbol indicates a Δ*cobA* strain synthesizing a plasmid-encoded CobA variant could not reach an OD_{630} of ≥1.0 after incubation in ethanolamine medium for 24 h at 37 °C. Individual doubling times as measured by optical density are as follows: 3.9 h for $CobA^{WT}$, no growth for $CobA^{F91A}$, no growth for $CobA^{F91W}$, no growth for $CobA^{F91H}$, 3.9 h for $CobA^{F91Y}$, no growth for $CobA^{F91D}$, no growth for $CobA^{W93A}$, 3.7 h for $CobA^{W93F}$, 24.2 h for $CobA^{W93H}$, 4.9 h for $CobA^{W93Y}$, no growth for $CobA^{W93D}$, no growth for $CobA^{F91A,W93A}$, and 3.7 h for $CobA^{F91W,W93F}$.

Consistent with the in vivo data, substitutions at Trp93 did not have a major effect on the activity of the enzyme, where the $CobA^{W93F}$, $CobA^{W93Y}$, and $CobA^{W93H}$ variants retained ≥78% of the specific activity of $CobA^{WT}$. The effect of a W93H substitution is noteworthy. Even though the in vitro specific activity of the $CobA^{W93H}$ variant with cob(II)alamin was only slightly lower (<10%) than that with $CobA^{WT}$, the $CobA^{W93H}$ variant only partially supported growth of the Δ*cobA* strain on ethanolamine (Figure 6A, group 2). To clarify this issue, we used a Co^+ assay to measure the combined rate of adenosylation and product release in a manner independent of those factors needed to generate the four-coordinate state. The variant $CobA^{W93H}$ only has 58% specific activity relative to that of the wild type in this assay, yet this value is still higher than those of several other CobA variants capable of complementation (Figure 7A). It is likely that the $CobA^{W93H}$ variant has a detrimental effect in vivo that is not evident in the in vitro assay. Further work is required to elucidate the effects of this variant on corrinoid adenosylation.

The effects of substitutions at position Phe91 were more severe than those at Trp93, which might be expected on the basis of the closer proximity of its side chain to the corrin ring. $CobA^{F91A}$, $CobA^{F91H}$, and $CobA^{F91D}$ variants lost >95% of their activity relative to that of $CobA^{WT}$ in the Co^{2+} assay. Surprisingly, a $CobA^{F91Y}$ variant retained sufficient enzymatic activity (85% of that of $CobA^{WT}$) to support growth of the Δ*cobA* strain on ethanolamine.

The effect of histidine in variant $CobA^{F91H}$ was very similar to that reported for the *Lr*PduO ACAT, where replacement of the critical Phe112 residue with histidine inactivated the enzyme by mimicking the effect of the coordination of the imidazole ring of DMB with the cobalt ion.[23] It is unknown whether the imidazole side chain of the $CobA^{F91H}$ variant interacts with the cobalt ion, but the predicted proximity of the side chain makes this likely.

Kinetic Analyses of CobA Variants. As described above, two assays were used to evaluate CobA activity in vitro. The first assay (termed the Co^{2+} assay) used a flavoprotein reductase (Fpr) and NADH to reduce cob(III)alamin to cob(I)alamin via reduced flavodoxin A (FldA). The latter is an electron transfer protein specifically recognized by CobA.[12,19] Reduced FldA supplies the electron needed to reduce cob(II)alamin to cob(I)alamin in the active site of CobA. Because the Co^{2+} assay measures the rates of reduction and adenosylation, we consider this assay to be more reflective of what happens in vivo.

The second assay (termed the Co^+ assay) bypasses the need for the Fpr/FldA system by chemically reducing cob(III)alamin to cob(I)alamin using Ti(III)citrate.[19] Cob(I)alamin is a four-coordinate species in solution[41] and needs only to be positioned adjacent to ATP to perform a nucleophilic attack on the 5′-carbon of ATP to yield AdoCbl and PPP_i.[21] With the exception of $CobA^{F91D}$, all CobA variants had detectable activity with the Co^+ assay (Figure 7A and Table 2). Furthermore, the K_M values of all other variant proteins were <5-fold different than those of $CobA^{WT}$ with respect to cob(I)alamin and ATP. The reason for the lack of activity in the $CobA^{F91D}$ variant is unknown, although placement of a polar, charged side chain in the proximity of several hydrophobic groups may be detrimental to protein function. Interestingly, the $CobA^{W93D}$ retains ∼40% specific activity relative to that of the wild type in the Co^+ assay, further indicating a greater tolerance for amino acid variation at this position.

In contrast to the Co^+ assay, the Co^{2+} assay showed a much greater variation in kinetic parameters among variants with ≥30% $CobA^{WT}$ activity (Table 3). The apparent Michaelis constant (K_M) values are higher for $CobA^{F91W}$, $CobA^{W93H}$, and $CobA^{F91W,W93F}$ than for $CobA^{WT}$, indicating that such substitutions affect the ability of the enzyme to bind the substrate under saturating conditions. Surprisingly, the cob(II)alamin K_M values of $CobA^{F91Y}$, $CobA^{W93F}$, and $CobA^{W93Y}$ were 3-, 4-, and 8-fold lower, respectively, than that of $CobA^{WT}$.

Turnover (k_{cat}) values were relatively unchanged across all variants, with the exception of 2- and 10-fold enhancements for $CobA^{F91Y}$ with respect to cobalamin and ATP, respectively, and a >10-fold decrease with respect to cob(II)alamin for $CobA^{F91W}$. Notable exceptions are discussed below.

dx.doi.org/10.1021/bi301378d | *Biochemistry* 2012, 51, 9647−9657

Table 2. Kinetic Parameters of Wild-Type CobA and Its Variants Using the Co^+ Assay[a]

	cob(I)alamin			ATP		
protein	K_M (μM)	k_{cat} (s^{-1})	k_{cat}/K_M (M^{-1} s^{-1})	K_M (μM)	k_{cat} (s^{-1})	k_{cat}/K_M (M^{-1} s^{-1})
$CobA^{WT}$	4 ± 1	(8 ± 1) × 10^{-2}	(2 ± 0.3) × 10^4	7 ± 2	(8 ± 1) × 10^{-2}	(1 ± 0.2) × 10^4
$CobA^{F91A}$	5 ± 1	(2 ± 0.1) × 10^{-2}	(4 ± 1) × 10^3	9 ± 4	(2 ± 0.1) × 10^{-2}	(2 ± 0.5) × 10^3
$CobA^{F91W}$	5 ± 2	(8.0 ± 1) × 10^{-2}	(2 ± 0.3) × 10^4	9 ± 2	(8 ± 1) × 10^{-3}	(9 ± 1) × 10^2
$CobA^{F91H}$	3 ± 1	(2 ± 1) × 10^{-2}	(5 ± 1) × 10^3	3 ± 0.4	(2 ± 0.5) × 10^{-2}	(6 ± 1) × 10^3
$CobA^{F91Y}$	1 ± 1	(5 ± 0.3) × 10^{-2}	(5 ± 2) × 10^4	0.3 ± 0.1	(5 ± 0.4) × 10^{-2}	(2 ± 0.4) × 10^5
$CobA^{F91D}$	ND[b]			ND[b]		
$CobA^{W93A}$	11 ± 4	(5 ± 0.5) × 10^{-2}	(4 ± 1) × 10^3	3 ± 0.5	(4 ± 0.2) × 10^{-2}	(2 ± 0.3) × 10^4
$CobA^{W93F}$	12 ± 5	(9 ± 1) × 10^{-3}	(8 ± 0.5) × 10^2	30 ± 9	(1 ± 0.1) × 10^{-2}	(3 ± 0.5) × 10^2
$CobA^{W93H}$	2 ± 0.3	(8 ± 0.5) × 10^{-2}	(4 ± 0.5) × 10^4	26 ± 10	(7 ± 0.3) × 10^{-2}	(3 ± 1) × 10^3
$CobA^{W93Y}$	16 ± 7	(9 ± 1) × 10^{-3}	(6 ± 2) × 10^2	2 ± 0.4	(1 ± 0.1) × 10^{-1}	(7 ± 1) × 10^3
$CobA^{W93D}$	2 ± 0.4	(5 ± 0.1) × 10^{-2}	(2 ± 0.3) × 10^4	3 ± 1	(5 ± 0.2) × 10^{-2}	(2 ± 0.3) × 10^4
$CobA^{F91A,W93A}$	3 ± 1	(1 ± 0.2) × 10^{-2}	(5 ± 1) × 10^3	2 ± 0.6	(8 ± 1) × 10^{-3}	(5 ± 1) × 10^3
$CobA^{F91W,W93F}$	9 ± 4	(4 ± 0.3) × 10^{-3}	(4 ± 1) × 10^2	6 ± 2	(1 ± 0.1) × 10^{-2}	(2 ± 1) × 10^3

[a]The cob(I)alamin was generated chemically using Ti(III)citrate as the reductant. [b]Not determined because of low activity.

Table 3. Kinetic Parameters of Wild-Type CobA and Its Variants Using the Co^{2+} Assay[a]

	cob(II)alamin			ATP		
protein	K_M (μM)	k_{cat} (s^{-1})	k_{cat}/K_M (M^{-1} s^{-1})	K_M (μM)	k_{cat} (s^{-1})	k_{cat}/K_M (M^{-1} s^{-1})
$CobA^{WT}$	25 ± 5	(6 ± 0.9) × 10^{-3}	(2 ± 0.4) × 10^2	66 ± 18	(5 ± 0.7) × 10^{-3}	(8 ± 2) × 10
$CobA^{F91A}$	ND[b]			ND[b]		
$CobA^{F91W}$	152 ± 40	(9 ± 1) × 10^{-4}	(6 ± 1) × 10^0	3 ± 0.8	(1 ± 0.1) × 10^{-3}	(4 ± 1) × 10^2
$CobA^{F91H}$	ND[b]			ND[b]		
$CobA^{F91Y}$	9 ± 0.1	(2 ± 0.4) × 10^{-2}	(2 ± 0.1) × 10^3	38 ± 9	(1 ± 0.1) × 10^{-2}	(3 ± 0.5) × 10^2
$CobA^{F91D}$	ND[b]			ND[b]		
$CobA^{W93A}$	ND[b]			ND[b]		
$CobA^{W93F}$	3 ± 0.4	(3 ± 0.4) × 10^{-3}	(1 ± 0.2) × 10^3	3 ± 0.5	(4 ± 0.4) × 10^{-3}	(1 ± 0.2) × 10^3
$CobA^{W93H}$	56 ± 15	(6 ± 2) × 10^{-3}	(1 ± 0.2) × 10^2	15 ± 5	(3 ± 0.4) × 10^{-3}	(2 ± 0.5) × 10^2
$CobA^{W93Y}$	4 ± 0.3	(7 ± 1) × 10^{-3}	(2 ± 0.1) × 10^4	79 ± 20	(6 ± 2.0) × 10^{-3}	(7 ± 1) × 10
$CobA^{W93D}$	ND[b]			ND[b]		
$CobA^{F91A,W93A}$	ND[b]			ND[b]		
$CobA^{F91W,W93F}$	38 ± 14	(7 ± 0.4) × 10^{-3}	(2 ± 0.4) × 10^2	33 ± 11	(4 ± 0.7) × 10^{-3}	(1 ± 0.4) × 10^2

[a]All measurements were generated in duplicate; the error corresponds to the standard deviation from the arithmetic mean. [b]Not determined because of the low activity.

While the specific activity of $CobA^{WT}$ increased >30-fold when cob(I)alamin was used as a substrate, other variants increased only a few-fold over their specific activity with cob(II)alamin (Figure 7). Kinetic parameters indicated that many of the variants with <10% of the $CobA^{WT}$ activity also had 10−15-fold lower catalytic efficiencies with respect to ATP (Table 3). Explanations for these observations are not obvious from available data and need to be investigated further.

Effect of an F91W Substitution on CobA Activity. The formation of four-coordinate cob(II)alamin requires a hydrophobic residue of sufficient bulk to displace the α-ligand base. Given that the activity of the $CobA^{F91W,W93F}$ variant was similar to that of $CobA^{WT}$ in the Co^{2+} assay (Figures 5 and 6), we hypothesized that $CobA^{F91W}$ might also exhibit high levels of activity. Surprisingly, the $CobA^{F91W}$ variant had a >10-fold decrease in k_{cat} values and >10-fold increase in K_M for cob(II)alamin relative to those of $CobA^{WT}$. The $CobA^{F91W}$ variant also failed to support growth of a Δ*cobA* strain (Figure 5A). In contrast, K_M values for ATP were lower than those of $CobA^{F91W}$, and the turnover number was only a few-fold lower than that of $CobA^{WT}$ in the Co^{2+} assay. Collectively, these data suggest that the F91W replacement affects cob(II)alamin binding or the formation of four-coordinate cob(II)alamin. Kinetic data obtained using the Co^+ assay (Table 2) support the possibility that smaller ligand base displacement is the process affected by this replacement, because the kinetic values for $CobA^{F91W}$ did not differ significantly from those of $CobA^{WT}$. This information suggests that binding of cob(I)alamin to $CobA^{F91W}$ is not impaired, but because cob(I)alamin is a four-coordinate species, the reaction can occur as efficiently as in $CobA^{WT}$.

The F91Y Substitution Makes the *S. enterica* CobA a Better Enzyme in Vitro. Strikingly, one CobA variant was a better enzyme than $CobA^{WT}$ in vitro in both the Co^+ and Co^{2+} assays. In the Co^+ assay, the $CobA^{F91Y}$ variant had a ∼4-fold lower K_M for cob(I)alamin and an ∼20-fold lower K_M for ATP. In the more physiologically relevant Co^{2+} assay, the $CobA^{F91Y}$ variant displayed an ∼3-fold higher k_{cat} and an ∼10-fold higher catalytic efficiency (k_{cat}/K_M) than $CobA^{WT}$. These results were surprising because, on the basis of the structure, it would be predicted that the additional polar hydroxyl group might interfere with ligand binding, coordinate with the cobalt ion, or slow product formation or release. Bioinformatic analysis[42] shows that residue Phe91 is conserved among members of the CobA family (Figure S1 of the Supporting Information). Several species of the genus *Ralstonia* have a tyrosine in place of phenylalanine in the equivalent residue of their putative CobA proteins. Several species, including the plant pathogen *Ralstonia*

dx.doi.org/10.1021/bi301378d | *Biochemistry* 2012, 51, 9647−9657

solanacearum, contain the complete suite of AdoCbl biosynthetic genes, several B_{12}-dependent enzymes, and additional ACATs.[43] To the best of our knowledge, this is the only variation of this residue tolerated in nature, but this does not explain why this variant has improved kinetic parameters or why it is not seen more frequently.

CONCLUSIONS

The structure and mutational and kinetic analyses of the housekeeping CobA ACAT of *S. enterica* in complex with cob(II)alamin and MgATP offer new insights into its mechanism of catalysis. The structure also revealed how the catalytically important four-coordinate cob(II)alamin intermediate binds to the active site of the enzyme. Although CobA- and PduO-type ACATs are structurally dissimilar, both types of enzymes use similar mechanisms to accomplish corrinoid adenosylation. In CobA, smaller ligand base displacement appears to be the result of a coordinated effect of residues Phe91 and Trp93, neither of which can coordinate to the cobalt ion of the ring, bringing the redox potential of the Co^{2+}/Co^{+} pair within reach of the $FMNH_2$ cofactor of flavodoxin A (FldA). The importance of residues Phe91 and Trp93 was confirmed in vitro and in vivo.

ASSOCIATED CONTENT

Supporting Information

Strain tables, plasmid tables, extinction coefficients, and a multiple-sequence alignment plot. This material is available free of charge via the Internet at http://pubs.acs.org.

Accession Codes

X-ray coordinates for the cob(II)alamin·CobA complex have been deposited in the Research Collaboratory for Structural Bioinformatics as Protein Data Bank entry 4HUT.

AUTHOR INFORMATION

Corresponding Author

*J.C.E.-S.: Department of Microbiology, University of Georgia, 527 Biological Sciences Building, 120 Cedar St., Athens, GA 30602; phone, (706) 542-2651; Fax, (706) 542-2815; e-mail, jcescala@uga.edu. I.R.: Department of Biochemistry, University of Wisconsin, 433 Babcock Dr., Madison, WI 53706; phone, (608) 262-0437; fax, (608) 262-1319; e-mail, ivan_rayment@biochem.wisc.edu.

Funding

This work was supported by National Institutes of Health Grants R37 GM40313 to J.C.E.-S. and R01 GM083987 to I.R. T.C.M. was supported in part by Chemistry and Biology Interface Training (CBIT) Grant T32 GM008505. Use of the SBC BM19 beamline at the Argonne National Laboratory Advanced Photon Source was supported by the U.S. Department of Energy, Office of Energy Research, under Contract W-31-109-ENG-38.

Notes

The authors declare no competing financial interest.

ABBREVIATIONS

ACAT, ATP:co(I)rrinoid adenosyltransferase; Cbl, cobalamin; Coα, cobalamin α-ligand; Coβ, cobalamin β-ligand; DMB, 5,6-dimethylbenzimidazole; Cbl, cobalamin; Cbi, cobinamide; AdoCbl, adenosylcobalamin; CoB_{12}, coenzyme B_{12}; HOCbl, hydroxycobalamin; PPP_i, tripolyphosphate; *Lr*PduO, *L. reuteri* PduO; Tris-HCl, tris(hydroxymethyl)aminomethane hydrochloride; TCEP, tris(2-carboxyethyl)phosphine; rTEV, recombinant tobacco etch virus; NTA, nitrilotriacetic acid; FAD, flavin adenine dinucleotide; FldA, flavodoxin A; Fpr, ferredoxin (flavodoxin):NADPH reductase; NADH, reduced nicotinamide adenine dinucleotide; MES, 2-(*N*-morpholino)-ethanesulfonic acid.

REFERENCES

(1) Warren, M. J., Raux, E., Schubert, H. L., and Escalante-Semerena, J. C. (2002) The biosynthesis of adenosylcobalamin (vitamin B12). *Nat. Prod. Rep. 19*, 390−412.

(2) Randaccio, L., Geremia, S., Demitri, N., and Wuerges, J. (2010) Vitamin B12: Unique metalorganic compounds and the most complex vitamins. *Molecules 15*, 3228−3259.

(3) Lenhert, P. G., and Hodgkin, D. C. (1961) Structure of the 5,6-dimethylbenzimidazolylcobamide coenzyme. *Nature 192*, 937−938.

(4) Babior, B. M. (1970) The mechanism of action of ethanolamine ammonia-lyase, a B12-dependent enzyme. VII. The mechanism of hydrogen transfer. *J. Biol. Chem. 245*, 6125−6133.

(5) Toraya, T. (2002) Enzymatic radical catalysis: Coenzyme B12-dependent diol dehydratase. *Chem. Rec. 2*, 352−366.

(6) Banerjee, R., and Vlasie, M. (2002) Controlling the reactivity of radical intermediates by coenzyme B_{12}-dependent methylmalonyl-CoA mutase. *Biochem. Soc. Trans. 30*, 621−624.

(7) Escalante-Semerena, J. C., Suh, S. J., and Roth, J. R. (1990) *cobA* function is required for both de novo cobalamin biosynthesis and assimilation of exogenous corrinoids in *Salmonella typhimurium*. *J. Bacteriol. 172*, 273−280.

(8) Johnson, M. G., and Escalante-Semerena, J. C. (1992) Identification of 5,6-dimethylbenzimidazole as the *Co*α ligand of the cobamide synthesized by *Salmonella typhimurium*. Nutritional characterization of mutants defective in biosynthesis of the imidazole ring. *J. Biol. Chem. 267*, 13302−13305.

(9) Buan, N. R., Suh, S. J., and Escalante-Semerena, J. C. (2004) The *eutT* gene of *Salmonella enterica* encodes an oxygen-labile, metal-containing ATP:corrinoid adenosyltransferase enzyme. *J. Bacteriol. 186*, 5708−5714.

(10) IUPAC-IUB Commission on Biochemical Nomenclature (1974) The nomenclature of corrinoids (1973 recommendations). *Biochemistry 13*, 1555−1560.

(11) Mera, P. E., and Escalante-Semerena, J. C. (2010) Multiple roles of ATP:cob(I)alamin adenosyltransferases in the conversion of B_{12} to coenzyme B_{12}. *Appl. Microbiol. Biotechnol. 88*, 41−48.

(12) Fonseca, M. V., and Escalante-Semerena, J. C. (2001) An in vitro reducing system for the enzymic conversion of cobalamin to adenosylcobalamin. *J. Biol. Chem. 276*, 32101−32108.

(13) Olteanu, H., Wolthers, K. R., Munro, A. W., Scrutton, N. S., and Banerjee, R. (2004) Kinetic and thermodynamic characterization of the common polymorphic variants of human methionine synthase reductase. *Biochemistry 43*, 1988−1997.

(14) Lexa, D., and Saveant, J.-M. (1983) The electrochemistry of vitamin B12. *Acc. Chem. Res. 16*, 235−243.

(15) Stich, T. A., Brooks, A. J., Buan, N. R., and Brunold, T. C. (2003) Spectroscopic and computational studies of Co^{3+}-corrinoids: Spectral and electronic properties of the B_{12} cofactors and biologically relevant precursors. *J. Am. Chem. Soc. 125*, 5897−5914.

(16) Stich, T. A., Buan, N. R., and Brunold, T. C. (2004) Spectroscopic and computational studies of Co^{2+}corrinoids: Spectral and electronic properties of the biologically relevant base-on and base-off forms of Co^{2+}cobalamin. *J. Am. Chem. Soc. 126*, 9735−9749.

(17) Park, K., Mera, P. E., Escalante-Semerena, J. C., and Brunold, T. C. (2008) Kinetic and spectroscopic studies of the ATP:corrinoid adenosyltransferase PduO from *Lactobacillus reuteri*: Substrate specificity and insights into the mechanism of Co(II)corrinoid reduction. *Biochemistry 47*, 9007−9015.

(18) Stich, T. A., Buan, N. R., Escalante-Semerena, J. C., and Brunold, T. C. (2005) Spectroscopic and computational studies of the ATP:corrinoid adenosyltransferase (CobA) from *Salmonella enterica*:

Insights into the mechanism of adenosylcobalamin biosynthesis. *J. Am. Chem. Soc. 127*, 8710−8719.
(19) Buan, N. R., and Escalante-Semerena, J. C. (2005) Computer-assisted docking of flavodoxin with the ATP:co(I)rrinoid adenosyltransferase (CobA) enzyme reveals residues critical for protein-protein interactions but not for catalysis. *J. Biol. Chem. 280*, 40948−40956.
(20) Hoover, D. M., Jarrett, J. T., Sands, R. H., Dunham, W. R., Ludwig, M. L., and Matthews, R. G. (1997) Interaction of *Escherichia coli* cobalamin-dependent methionine synthase and its physiological partner flavodoxin: Binding of flavodoxin leads to axial ligand dissociation from the cobalamin cofactor. *Biochemistry 36*, 127−138.
(21) Fonseca, M. V., Buan, N. R., Horswill, A. R., Rayment, I., and Escalante-Semerena, J. C. (2002) The ATP:co(I)rrinoid adenosyltransferase (CobA) enzyme of *Salmonella enterica* requires the 2′-OH group of ATP for function and yields inorganic triphosphate as its reaction byproduct. *J. Biol. Chem. 277*, 33127−33131.
(22) Bauer, C. B., Fonseca, M. V., Holden, H. M., Thoden, J. B., Thompson, T. B., Escalante-Semerena, J. C., and Rayment, I. (2001) Three-dimensional structure of ATP:corrinoid adenosyltransferase from *Salmonella typhimurium* in its free state, complexed with MgATP, or complexed with hydroxycobalamin and MgATP. *Biochemistry 40*, 361−374.
(23) Mera, P. E., St Maurice, M., Rayment, I., and Escalante-Semerena, J. C. (2009) Residue Phe112 of the human-type corrinoid adenosyltransferase (PduO) enzyme of *Lactobacillus reuteri* is critical to the formation of the four-coordinate Co(II) corrinoid substrate and to the activity of the enzyme. *Biochemistry 48*, 3138−3145.
(24) Ratzkin, P., and Roth, J. R. (1978) Cluster of genes controlling proline degradation in *Salmonella typhimurium*. *J. Bacteriol. 133*, 744−754.
(25) Balch, W. E., and Wolfe, R. S. (1976) New approach to the cultivation of methanogenic bacteria: 2-Mercaptoethanesulfonic acid (HS-CoM)-dependent growth of *Methanobacterium ruminantium* in a pressurized atmosphere. *Appl. Environ. Microbiol. 32*, 781−791.
(26) Bertani, G. (1951) Studies on lysogenesis. I. The mode of phage liberation by lysogenic *Escherichia coli*. *J. Bacteriol. 62*, 293−300.
(27) Bertani, G. (2004) Lysogeny at mid-twentieth century: P1, P2, and other experimental systems. *J. Bacteriol. 186*, 595−600.
(28) Gasteiger, E., Gattiker, A., Hoogland, C., Ivanyi, I., Appel, R. D., and Bairoch, A. (2003) ExPASy: The proteomics server for in-depth protein knowledge and analysis. *Nucleic Acids Res. 31*, 3784−3788.
(29) Rocco, C. J., Dennison, K. L., Klenchin, V. A., Rayment, I., and Escalante-Semerena, J. C. (2008) Construction and use of new cloning vectors for the rapid isolation of recombinant proteins from *Escherichia coli*. *Plasmid 59*, 231−237.
(30) Blommel, P. G., and Fox, B. G. (2007) A combined approach to improving large-scale production of tobacco etch virus protease. *Protein Expression Purif. 55*, 53−68.
(31) Otwinowski, Z., and Minor, W. (1997) Processing of X-ray diffraction data collected in oscillation mode. *Methods Enzymol. 276*, 307−326.
(32) Vagin, A., and Teplyakov, A. (2000) An approach to multi-copy search in molecular replacement. *Acta Crystallogr. D56*, 1622−1624.
(33) Emsley, P., and Cowtan, K. (2004) Coot: Model-building tools for molecular graphics. *Acta Crystallogr. D60*, 2126−2132.
(34) Murshudov, G. N., Vagin, A. A., Lebedev, A., Wilson, K. S., and Dodson, E. J. (1999) Efficient anisotropic refinement of macromolecular structures using FFT. *Acta Crystallogr. D55* (Part 1), 247−255.
(35) St Maurice, M., Mera, P., Park, K., Brunold, T. C., Escalante-Semerena, J. C., and Rayment, I. (2008) Structural characterization of a human-type corrinoid adenosyltransferase confirms that coenzyme B_{12} is synthesized through a four-coordinate intermediate. *Biochemistry 47*, 5755−5766.
(36) Fonseca, M. V., and Escalante-Semerena, J. C. (2000) Reduction of cob(III)alamin to cob(II)alamin in *Salmonella enterica* Serovar Typhimurium LT2. *J. Bacteriol. 182*, 4304−4309.
(37) Ouyang, L., Rulis, P., Ching, W. Y., Nardin, G., and Randaccio, L. (2004) Accurate redetermination of the X-ray structure and electronic bonding in adenosylcobalamin. *Inorg. Chem. 43*, 1235−1241.
(38) Marsh, E. N., and Harding, S. E. (1993) Methylmalonyl-CoA mutase from *Propionibacterium shermanii*: Characterization of the cobalamin-inhibited form and sububit-cofactor interactions studied by analytical ultracentrifugation. *Biochem. J. 290*, 551−555.
(39) Roof, D. M., and Roth, J. R. (1992) Autogenous regulation of ethanolamine utilization by a transcriptional activator of the *eut* operon in *Salmonella typhimurium*. *J. Bacteriol. 174*, 6634−6643.
(40) Liu, D., Williamson, D. A., Kennedy, M. L., Williams, T. D., Morton, M. M., and Benson, D. R. (1999) Aromatic side chain-porphyrin interactions in designed hemoproteins. *J. Am. Chem. Soc. 121*, 11798−11812.
(41) Wirt, M. D., Sagi, I., and Chance, M. R. (1992) Formation of a square-planar cobalt(I) B-12 intermediate: Implication for enzyme catalysis. *Biophys. J. 63*, 412−417.
(42) Altschul, S. F., Gish, W., Miller, W., and Myers, E. W. (1990) Basic local alignment search tool. *J. Mol. Biol. 215*, 403−410.
(43) Rodionov, D. A., Vitreschak, A. G., Mironov, A. A., and Gelfand, M. S. (2003) Comparative genomics of the vitamin B_{12} metabolism and regulation in prokaryotes. *J. Biol. Chem. 278*, 41148−41159.
(44) DeLano, W. L. (2002) *The Pymol Molecular Graphics System*, DeLano Scientific, San Carlos, CA.